Power Dispatch Strategy for Interconnected Microgrids Based Hybrid Renewable Energy System

Marwa Grami*, Mouna Rekik*, Lotfi Krichen*

* Department of Electrical Engineering, National Engineering School of Sfax, University of Sfax, Control and Energy Management Laboratory (CEM_Lab) BP 1173, 3038, Sfax, Tunisia

(gramimarwa@gmail.com, mouna_ing@hotmail.fr, lotfi.krichen@enis.tn)

Corresponding Author; Marwa GRAMI, National Engineering School of Sfax, Control and Energy Management Laboratory (CEM_Lab) BP 1173, 3038, Sfax, Tunisia, Tel.: (+216) 74 274 418 / Fax: (+216) 74 275 595, gramimarwa@gmail.com

Received: 17.01.2018 Accepted:26.02.2018

Abstract- This paper proposes a studied system made up of interconnected microgrids (MGs) in which each one includes a hybrid renewable energy system (HRES). The proposed power dispatch strategy ensures load satisfaction in each MG by maintaining the equilibrium between production and consumer demand power via interactions among MGs and the utility grid. The purpose of this paper is to provide an adequate supply to the different MGs by adapting production to consumption according to the available hybrid power production. This is done with the consideration of the dispatch of the power exchanged among MGs and the main grid. The cooperation between the multiples MGs ensures higher resilience and flexibility of the whole distribution system. The proposed method not only maximizes the use of RES production, but also realizes the managing of multi energy sources under different scenarios of power generation and load demand in each MG. The results of the studied case are provided to show the feasibility of this proposed power dispatch strategy in the smart grid environment.

Keywords MGs, HRES, power dispatch strategy, load satisfaction, smart grid.

1. Introduction

Smart grid can be described as an intelligent grid operating at larger utility grid level such as large distribution lines and transmission. Microgrid (MG) attracts considerable attention in the smart grid environment as a smaller scale with the ability of operating independently from the larger utility grid [1-3]. The MG can be a combination of sources like renewable sources, storage systems and diesel generators forming a hybrid renewable energy system (HRES) to satisfy the local loads [4].

In the literature, several approaches have studied the concept of a single MG. Some of them focused on the operation of a single MG without integrating multiples energies [5,6]. Others proposed a method of optimal coordinated energy dispatch for a multi energy MG [7]. A dynamic operation and control approach for a MG hybrid power systems were developed in [8]. A distributed economic dispatch approach for a MG with a high renewable energy penetration was proposed in [9,10]. The MG can operate either in autonomous or in a grid-connected mode [11]. In stand-alone mode, the MG feeds power to the internal load demand [12,13]. In grid-connected mode, authors in [14,15] developed energy management strategies for a MG connected to the main grid . However, only one single MG was studied in the above works.

On the other hand, many researches worked on the study of multiple MGs. Some of them focused on the single energy dispatch for islanded MGs [16-19]. Others worked on the optimization technique to get the load dispatch of MGs [20]. For the [21], the use of MGs in enhancing energy security and resilience was discussed. However, the communication between the multiple MGs was not studied.

Other researches focused on the optimal power dispatch between the interconnected MGs taking in consideration different possible interactions. Authors in [22] presented a cooperative energy dispatch strategy considering interactions between distributed renewable sources and storage for multiple autonomous MGs. In ref [23], several MGs interact by exchanging energy in order to satisfy their local demand while minimizing the global cost. But, these previous works have presented approaches to ensure load satisfaction focusing on interaction between MGs without studying the communication with the main grid.

Other researches worked on load satisfaction for optimal operating of the main grid. Authors in [24] studied the interaction between MGs and the grid to get a decentralized energy management system. A power dispatching strategy has considered interaction between MGs and the grid with the objective of minimizing operational cost in distributed smart grid [25]. In [26], a multi MGs approach was proposed for optimal operating of the active distribution networks. However, these previous approaches focused on interaction between MGs and the main grid without taking into account the communication between the interconnected MGs.

All these methods have proposed good solutions to ensure load satisfaction but each of them focuses on a specific objective task without considering the simultaneous interactions and data transfer between the distributed power sources in each MG, between the neighboring MGs and between the multiple MGs and the main grid.

For that, in this study, a power dispatch strategy is presented to monitor the multiple MGs with the grid in eleven modes, to ensure power dispatch and to maintain the power equilibrium between production and consumption power. This is done considering the communication and the data transfer between the neighboring MGs and between the interconnected MGs and the main grid. Each MG includes a hybrid power system composed of RES (wind and solar), LI-ion batteries and a diesel generator. The main contribution of this work is to propose a power dispatch strategy according to the following constraints: (i) load demand, (ii) availability of multi energy resources, (iii) grid stability. The considered approach offers many power flow possibilities to monitor the MG in eleven operation modes providing more flexibility for the operation of each MG, maximizing the use of RES production and enhancing the whole studied system reliability. The focus of this considered strategy is firstly to maintain the equilibrium between the power generation and the load demand in each MG, and secondly to guarantee the interactions among MGs and the main grid with the exploitation of shared power between neighboring MGs and the main grid.

The remaining of this article is organized as follows. In section 2, the studied system is described. The model of the system components is developed in section3. In section 4, the proposed power management algorithm is explained in details. Simulation results are developed in section 5 and finally, the conclusion is given in section 6.

2. Studied System Description

The architecture of the studied system is presented in Fig. 1. It is made up of n interconnected MGs. Each one includes a hybrid renewable energy system (HRES) consisting of wind farm, photovoltaic generator, Li-ion battery and a diesel generator. Each MG is able to interchange power with the neighboring MGs and also with the main grid . The RES are used to power internal loads of each MG and also used to feed the needed power in the neighboring MGs. In case the RES are unavailable due to their intermittent and fluctuating behavior caused by the change climate conditions, the Li-ion battery reinforces the RES and also helps to provide the needed power of the neighboring MGs loads. The li-ion battery was selected in this work because the cell battery has high specific power and long lifetime. When no or little RES and Li-ion battery power are available, the role of the grid is to recover any needed power or to receive any excess power without disturbing the grid stability. Otherwise, the diesel generator (DG) is used as power supplying of the needed power.

3. Models of System Components

3.1. Wind farm model

In this work, similar wind turbine units (WT) with a short distance between them compose the studied wind farm (WF). The profiles of the wind speed applied to the considered unit are near and the WF is simulated with a large number of identical WT units. In order to increase the simulation speed, an aggregate model which consists of one equivalent WT can represent the WF. As input, the main value of wind speed applied to the equivalent WT is given by the following expression [27]:

$$V = \frac{\sum_{i=1}^{n_T} V_i}{n_T} \quad (1)$$

The actual output power of the equivalent WT can be calculated as follows [28]:

$$P_W(V) = \begin{cases} 0, & V < V_c \text{ or } V > V_F \\ \frac{V^2 - V_c^2}{V_R^2 - V_c^2}.\, P_{Wr}, & V_c \leq V \leq V_R \\ P_{Wr}, & V_R \leq V \leq V_F \end{cases} \quad (2)$$

3.2. Photovoltaic generator model

In this work, a simplified simulation model of the photovoltaic generator (PV generator) is presented to get the hourly output power estimation of the PV generator. The PV generator power is defined as follows [29, 30]:

$$P_{PV} = N_{PV}.\, \mu_{PV}.\, A_{PV}.\, GI \quad (3)$$

μ_{PV} is the PV generator efficiency expressed as:

$$\mu_{PV} = \mu_r.[1\text{-}\beta.(T_c - T_{cref})] \quad (4)$$

T_c is determined using the N_{oct} (Normal Operating Cell Temperature); it can be given by the following expression:

$$T_c = T_a + GI.\frac{N_{oct} - 20}{800} \quad (5)$$

Those different parameters are given by the PV module manufacturers.

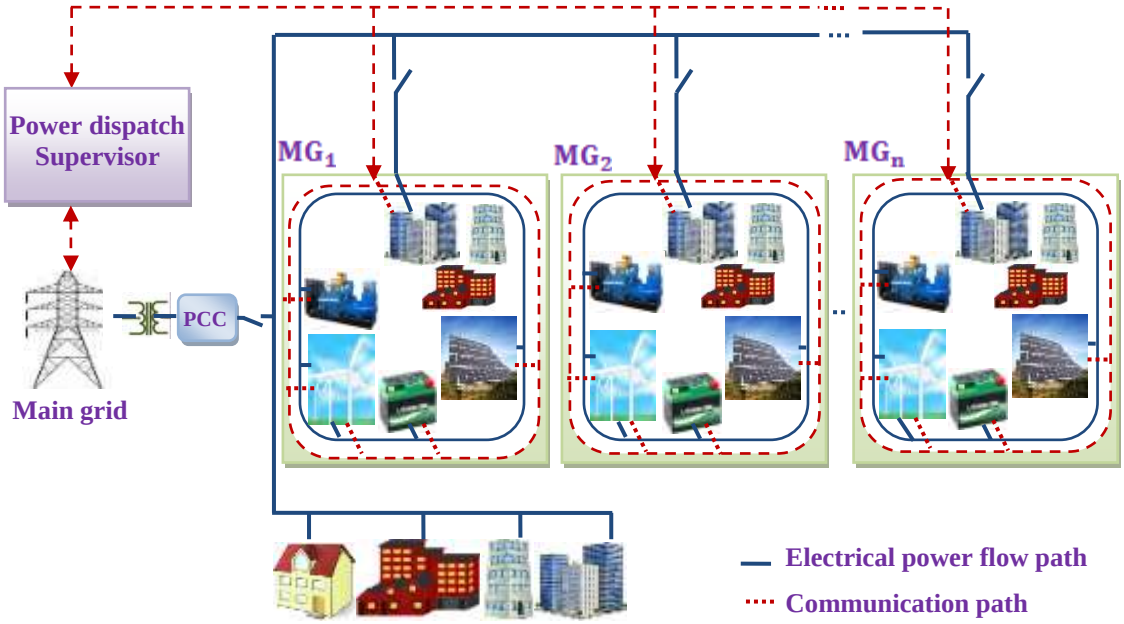

Fig.1. Studied system architecture.

3.3. Battery model

A voltage source V_{batt} connected in series with an internal resistance can be considered as the simplest model of an electrical battery. In charging mode, the voltage source of the Li-ion battery is defined as follows [31]:

$$V_{batt} = U_0 - R.i - K.\frac{Q}{i.t - 0.1.Q}i^* - K\frac{Q}{Q - i.t}i.t + Ae^{-B.i.t} \quad (6)$$

In discharging mode, the expression of the voltage source of the Li-ion battery is presented as follows [31]:

$$V_{batt} = U_0 - R.i - K.\frac{Q}{i.t - i.t}i^* - K\frac{Q}{Q - i.t}i.t + Ae^{-B.i.t} \quad (7)$$

The equation of the state of charge (SOC) is expressed as [32]:

$$SOC=100(1-\frac{i.t}{Q}). \quad (8)$$

3.4. Diesel generator model

The DG is currently used in diverse applications [33]. A diesel engine associated with a synchronous generator composes it. The torque T_d linked to the DG is given in the following equation [34, 35]:

$$T_d = \frac{F}{1+\tau_C.s}e^{-\tau_d.s} \quad (9)$$

4. Proposed Power Management Algorithm

In order to ensure a power dispatching between the different MGs and to manage the energy flow distribution, a power dispatch algorithm is proposed in Fig. 2. This algorithm allows the communication between the different MGs and the control of multi-source powers in each MG according to different constraints.

There are n MGs indexed by "i=1,2,…,n". In each MG_i, in order to meet the load demand and satisfy its power requirement, the PV_i and WF_i generators work together because of their complementary nature of produced powers. The RES_i produced power is calculated at each instant "t" as follows:

$$P_{RESi}(t)=P_{PVi}(t)+P_{WFi}(t) \quad (10)$$

This algorithm works as shown below :

The proposed algorithm allows calculating the power variation "$\Delta P_{i0}(t)$" by subtracting the RES generated power "$P_{RESi}(t)$" from the load required power "$P_{Li}(t)$" in MG_i. Its value can be a zero power, which means that the power equilibrium is well maintained or it can be a lack or an excess of power which must be compensated or absorbed in order to ensure the equilibrium between production and consumption power in MG_i.

This algorithm is divided into two parts. The first part is obtained in case of a lack of power and is divided into 5 sections (S1 → S5). The second part is realized in case of power excess and is divided into 5 sections (S6 → S10). Sections of each part are classified in order of priority.

When "$\Delta P_{i0}(t) > 0$", meaning that there is a lack of power in MG_i which must be compensated by the available production power. The first step is to verify if the neighboring MG_c indexed by "c=i+1,…,n" can afford the needed power without disturbing its own equilibrium between production and consumption power. The following iterative procedure will be continued until they afford the needed power, a part of it or nothing. The considered initializations are "$\Delta P_{i1}(t)=\Delta P_{i0}(t)$" and "c=i+1". If "$c \leq n$", the RES generated power "$P_{REScc}(t)$" will be compared with

the load required power "$P_{Lc}(t)$" in the MG_c as shown in Fig.2 - S1. When "$P_{RESc}(t) > P_{Lc}(t)$", the RES generated power in

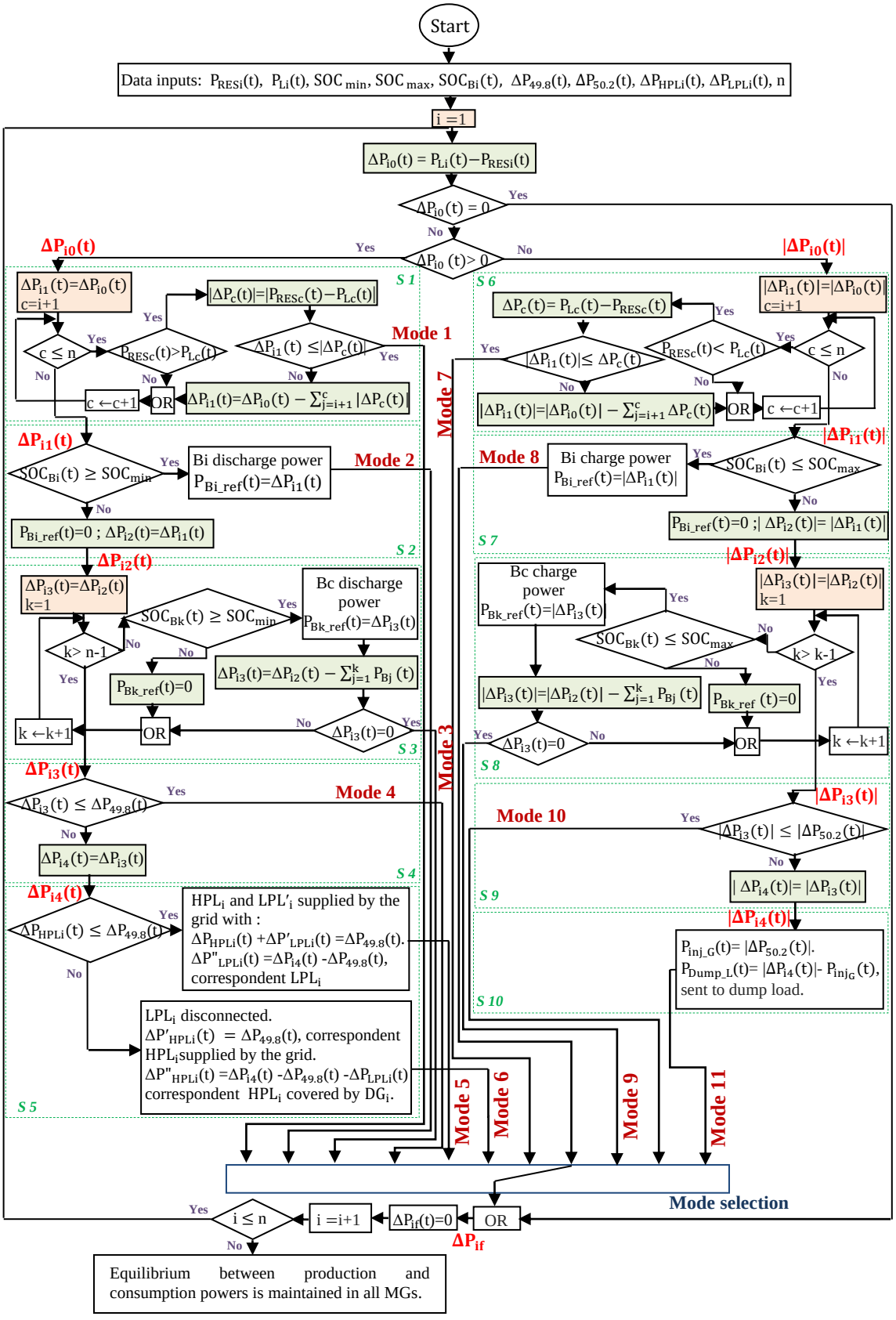

Fig.2. Proposed Power dispatch algorithm.

the MG_c can satisfy its own load power requirements and have an excess of power calculated as "$|\Delta P_c(t)|=|P_{RESc}(t)-P_{Lc}(t)|$" and compared with the required power "$\Delta P_{i1}(t)$". When "$\Delta P_{i1}(t) \leq |\Delta P_c(t)|$", meaning that the excess of power in the MG_c can compensate the needed power "$\Delta P_{i1}(t)$", the MG_i is satisfied with the neighboring MG_c power excess. This is the case of mode 1. If "$\Delta P_{i1}(t)>|\Delta P_c(t)|$", meaning that the neighboring MG_c can achieve only a part of the required power, the required power in MG_i decreases and its new value is given by the relation "$\Delta P_{i1}(t)=\Delta P_{i0}(t) - \sum_{j=i+1}^{c} |\Delta P_c(t)|$". If "$P_{RESc}(t) \leq P_{Lc}(t)$", meaning that the neighboring MG_c also has a lack of power, the MG_c cannot participate in providing the needed power to the MG_i. Due to these two latter cases, the MG_i is not satisfied and the next neighboring MG will be tested. These iterative tests are continued until verifying all neighboring MGs and finishing with an operating mode 1 or a required power "$\Delta P_{i1}(t)$" then passing to the next step.

If "$c > n$", the next step is to verify the available storage power of the MG_i as shown in Fig.2 - S2. In fact, when "$SOC_{Bi}(t) \geq SOC_{min}$", this is the mode of power storage discharging in the MG_i. The battery B_i acts to compensate the lack of power"$\Delta P_{i1}(t)$" by discharging power "$P_{Bi\_ref}(t)=\Delta P_{i1}(t)$". So, "$\Delta P_{i1}(t) = 0$" and the MG_i is satisfied by the discharge operation of its own battery, this is the case of mode 2. When "$SOC_{Bi}(t) < SOC_{min}$", meaning that the battery B_i reaches the minimum state of charge "SOC_{min}" and cannot participate in feeding the power variation "$\Delta P_{i1}(t)$". Thus, "$P_{Bi\_ref}(t)=0$", "$\Delta P_{i2}(t)= \Delta P_{i1}(t)$" and then the MG_i is not satisfied.

After testing the available storage power of the battery B_i and having the result that the MG_i is still in need of power, the available storage power of each neighboring MG_k will be verified in the next step as shown in Fig.2 - S3. There are k neighboring MGs with "k=1,…,n-1". The following iterative procedure will be continued until verifying all the available storage power of neighboring MGs and finishing with providing the needed power or nothing. The considered initializations are "$\Delta P_{i3}(t)=\Delta P_{i2}(t)$" and "k=1". If "$k \leq$ n-1" and "$SOC_{Bk}(t) \geq SOC_{min}$", meaning that the storage is accessible for the discharging of power until the minimum state of charge 'SOC_{min}' is reached and "$P_{Bk\_ref}(t)=\Delta P_{i3}(t)$", the new value of lack of power is "$\Delta P_{i3}(t)=\Delta P_{i2}(t) - \sum_{j=1}^{k} P_{Bj}(t)$". If "$\Delta P_{i3}(t) =0$", the required power in the MG_i is completely satisfied by the discharge operation of the neighboring battery B_k and this is the case of mode 3. The available storage power of the next neighboring MG will be verified in two cases: first when "$\Delta P_{i3}(t)\neq 0$" which means that the needed power of MG_i is not completely compensated by the battery B_k discharge power and second when "$k \leq$ n-1" and "$SOC_{Bk}(t) < SOC_{min}$" which means that the battery B_k expects the minimum state of charge 'SOC_{min}' and "$P_{Bk\_ref}(t)=0$". These iterative tests are continued until verifying all the available storage power of neighboring MGs and finishing with an operating mode 3 or a lack of power "$\Delta P_{i3}(t)$" and passing to the next step when "k>n-1".

The operating modes 4,5,6 will appear when the needed power of the MG_i is not fulfilled neither by any of its neighboring MGs intervention (RES power excess or storage discharging power) nor by its own storage discharging power.

"$\Delta P_{49.8}(t)$" is the power grid absorption corresponding to the 49.8 Hz frequency. The exchange of "$\Delta P_{49.8}(t)$" between the grid and the MGs should be assured without disturbing the grid stability and maintaining the frequency in the desired range. This power is presented in the following relation [27]:

$$\Delta P_{49.8}(t)=P_{GCL-max}(t)-P_{GCL}(t) \quad (11)$$

As shown in Fig.2 - S4, the algorithm compares its value with the power deficiency "$\Delta P_{i3}(t)$". If "$\Delta P_{i3}(t) \leq \Delta P_{49.8}(t)$", the grid power can supply the required power of the MG_i without disturbing the grid stability. Then, "$\Delta P_{i3}(t)=0$" and the MG_i is satisfied with the power absorption from the grid. This is the case of mode 4. When "$\Delta P_{i3}(t) > \Delta P_{49.8}(t)$", the required power not fed is "$\Delta P_{i4}(t) = \Delta P_{i3}(t)$". In order not to surpass the grid frequency limit "49.8", the grid affords only the power equal to "$\Delta P_{49.8}(t)$". Because the priority loads must always be satisfied in whatever condition, the algorithm compares the power of high priority loads (HPLs) with the absorbed power from the grid in order to verify if the source of lack of power "$\Delta P_{i3}(t)$" is coming only from the HPLs or from both high and low priority loads (LPLs) as shown in Fig.2 -S5.

Mode 5 corresponds to the case when the power "$\Delta P_{HPLi}(t)$" is less than the absorbed power from the grid "$\Delta P_{49.8}(t)$", meaning that the HPLs and a part of the LPLs (whose power is "$\Delta P'_{LPLi}(t)$") are fed by the grid with "$\Delta P_{HPLi}(t)+\Delta P'_{LPLi}(t)=\Delta P_{49.8}(t)$".
"$\Delta P''_{LPLi}(t) = \Delta P_{i4}(t) - \Delta P_{49.8}(t)$" correspond to the remaining part of the LPLs which is disconnected.

Mode 6 corresponds to the case when the HPLs power is higher than the absorbed power from the grid. In fact, in order not to disturb the grid frequency, the power absorbed from the grid must not exceed "$\Delta P_{49.8}(t)$" and then, the HPLs are not completely satisfied with the grid power "$\Delta P_{49.8}(t)$". In that case, "$\Delta P'_{HPLi}(t) = \Delta P_{49.8}(t)$" and a part of the HPLs ($\Delta P''_{HPLi}(t)$) is still not fed together with the LPLs ($\Delta P_{LPLi}(t)$). Therefore, loads corresponding to the power "$\Delta P''_{HPLi}(t)=\Delta P_{i4}(t)-\Delta P_{49.8}(t)-\Delta P_{LPLi}(t)$" are covered by the DG_i power and loads corresponding to the power "$\Delta P_{LPLi}(t)$" are disconnected.

Now, treating the case when "$\Delta P_{i0}(t)<0$" which means that there is an excess of power in the MG_i. To get the equilibrium between production and consumption power, the first step is to verify if the neighboring MG_c indexed by "c=i+1,…,n" have a lack of power in order to meet the needed power by "$|\Delta P_{i0}(t)|$" as shown in Fig.2 -S6. The following iterative procedure will be continued until verifying that they absorb the excess of power "$|\Delta P_{i0}(t)|$", a part of it or nothing. The considered initializations are "$|\Delta P_{i1}(t)|=|\Delta P_{i0}(t)|$" and "c=i+1". If "$c \leq n$", it is necessary to compare the RES_c generated power "$P_{RESc}(t)$" with the load required power "$P_{Lc}(t)$". In fact, when "$P_{RESc}(t) < P_{Lc}(t)$", meaning that the neighboring MG_c has a required power "$\Delta P_c(t)= P_{Lc}(t) - P_{RESc}(t)$" which will be compared with the

excess of power "$|\Delta P_{i1}(t)|$". When "$|\Delta P_{i1}(t)| \leq \Delta P_c(t)$", the load of neighboring MG_c can absorb the excess of power which leads to a decrease of the required power "$\Delta P_c(t)$" and a power equilibrium in the MG_i by supplying the power lack with "$|\Delta P_c(t)|$". This is the case of mode 7. When "$|\Delta P_{i1}(t)| > \Delta P_c(t)$", the MG_i can afford the needed power in the neighboring MG_c but still has an excess of power presented as follows "$|\Delta P_{i1}(t)| = |\Delta P_{i0}(t)| - \sum_{j=i+1}^{c} \Delta P_c(t)$". Otherwise, when "$P_{RESc}(t) > P_{Lc}(t)$", the neighboring MG_c has an excess of power and cannot absorb "$|\Delta P_{i0}(t)|$". In these two latter cases in which the MG_i has an excess of power, the next neighboring MG_c will be tested and these iterative tests will be continued until verifying all neighboring MGs and finishing with getting mode 7 or an excess of power "$|\Delta P_{i1}(t)|$".

If "$c > n$", the next step is to verify the available storage power of the MG_i as shown in Fig.2 -S7. When "$SOC_{Bi}(t) \leq SOC_{max}$", the battery B_i absorbs the excess of power "$|\Delta P_{i1}(t)|$" charging its power "$P_{Bi\_ref}(t)=|\Delta P_{i1}(t)|$". As a consequence, the balance between production and consumption power in MG_i is ensured by the charge operation of its own battery. This is the case of mode 8. When the battery B_i expects the maximum state of charge "SOC_{max}", it cannot charge the excess of power of the MG_i and therefore "$P_{Bi\_ref}(t)=0$" and "$|\Delta P_{i2}(t)|=|\Delta P_{i1}(t)|$". Due to this case, the MG_i still has power excess "$|\Delta P_{i2}(t)|$".

Now, after testing the available storage power of the battery B_i and having the result that the MG_i has power excess, the available storage power of each neighboring MG_k will be verified in the next step as shown in Fig.2 -S8. There are k neighboring MGs with "k=1,…,n-1". The following iterative procedure will be continued until verifying all the available storage power of neighboring MGs and finishing with charging the battery B_k with the excess of power, a part of it or nothing. The considered initializations are "$|\Delta P_{i3}(t)|=|\Delta P_{i2}(t)|$" and "k=1". If "$k \leq n-1$" and when "$SOC_{Bk}(t) \leq SOC_{max}$", the excess of power "$|\Delta P_{i3}(t)|$" will be sent to the battery B_k. In fact, the battery B_k acts to absorb "$|\Delta P_{i3}(t)|$" by charging "$P_{Bk\_ref}(t)=|\Delta P_{i3}(t)|$". The new excess of power is "$|\Delta P_{i3}(t)|=|\Delta P_{i2}(t)| - \sum_{j=1}^{k} P_{Bj}(t)$". If "$|\Delta P_{i3}(t)| = 0$", the equilibrium between production and consumption power in MG_i is ensured by the charge operation of its neighboring battery B_k. This is the case of mode 9. If "$|\Delta P_{i3}(t)| \neq 0$", the excess of power of MG_i is not completely charged by the neighboring battery B_k. If "$SOC_{Bk}(t) > SOC_{max}$", the SOC limit is reached, "$P_{Bk\_ref}(t)=0$" and then the battery B_k cannot participate in absorbing the required power in MG_i. Due to these two latter cases, the MG_i still has an excess of power "$|\Delta P_{i3}(t)|$" and hence the next available storage power of neighboring MGs will be tested. These iterative tests will be continued until verifying all the available storage power of neighboring MGs and finishing with an operating mode 9 or an excess of power "$|\Delta P_{i3}(t)|$" and passing to the next step when "k>n-1".

The operating modes 10 and 11 will appear when the MG_i still has an excess of power not absorbed neither by the neighboring MGs (loads in need of power or charging power) nor by its own battery charging power.

"$\Delta P_{50.2}(t)$" is the power corresponding to the 50.2 Hz frequency. This power is presented in the following equation [27]:

$$\Delta P_{50.2}(t) = P_{GCL-min}(t) - P_{GCL}(t) \quad (12)$$

The exchange of "$|\Delta P_{50.2}(t)|$" between the grid and the MGs should be assured without disturbing the grid stability and maintaining the frequency in the desired range [27]. So, as shown in Fig.2 -S9, the power grid injection into the grid "$|\Delta P_{50.2}(t)|$" will be compared with the excess of power "$|\Delta P_{i3}(t)|$". When "$|\Delta P_{i3}(t)| \leq |\Delta P_{50.2}(t)|$", "$|\Delta P_{i3}(t)|$" can be injected into the grid without disturbing its frequency. As a consequence, the MG_i is satisfied with power injection into the grid and "$\Delta P_{i3}(t)=0$". In this situation, mode 10 is obtained. When "$|\Delta P_{i3}(t)| > |\Delta P_{50.2}(t)|$", the power excess of the MG_i is higher than the power which can be injected to the grid without exceeding the frequency 50.2 Hz and then the power excess of MG_i is formulated as "$|\Delta P_{i4}(t)|=|\Delta P_{i3}(t)|$". In fact, only a part of the excess of power is injected into the network without disturbing the grid stability ($P_{inj\_G}(t)= |\Delta P_{50.2}(t)|$). Consequently, the MG_i still has an excess of power which will be sent to the dump load ($P_{Dump\_L}(t)= |\Delta P_{i4}(t)| - P_{inj\_G}(t)$) as shown in Fig.2 S10. This is the case of mode 11.

Once the equilibrium between production and consumption power in MG_i is ensured ($\Delta P_{if}(t)=0$), the same steps will be treated for the next MG until testing all the MGs.

5. Simulation Results

The simulated case study is made up of 3 MGs integrated HRES (n=3). The details of HRES in each MG are given in table 1. The specifications of the wind turbines, the PV module and the Li-ion battery cell are listed in Tables 2, 3 and 4, respectively.

In order to evaluate the effectiveness of the proposed strategy and to validate the different power flow paths, the simulation of the case study is performed using Matlab-Simulink. The simulation is executed over a period of 24 h for a typical day. In normal conditions, the network produces 215 MW in order to feed its connected loads.

This proposed strategy is evaluated according to the following conditions:

- Wind speeds of MGs 1, 2, and 3 that curve between 7 and 13 m/s are shown in Fig. 3.
- WF powers of MGs 1, 2 and 3 are given by Fig. 4.
- Solar irradiations of MGs 1, 2 and 3 are illustrated in Fig. 5.
- PV powers of MGs 1, 2 and 3 are observed in Fig. 6.
-Load demand powers of MGs 1, 2 and 3 are shown in Fig. 7.

Fig. 8 shows the battery states of charge and the battery powers of MGs 1, 2 and 3.

Power variation assessment ("$\Delta P_{10}(t)$" → "$\Delta P_{11}(t)$" → "$\Delta P_{12}(t)$" → "$\Delta P_{13}(t)$" → "$\Delta P_{14}(t)$" → "$\Delta P_{1f}(t)$") in which the power path chosen for the MG_1 ensures its power equilibrium between production and consumer demand is illustrated in Fig. 9. Indeed, the power transition from "$\Delta P_{10}(t)$" to "$\Delta P_{11}(t)$" point out the intervention of the neighboring MGs 2 and 3 (with their RES power excess or their required power). The power transition from "$\Delta P_{11}(t)$" to "$\Delta P_{12}(t)$"

shows the intervention of the battery B_1 (with charge or discharge operations). The power transition from "$\Delta P_{12}(t)$" to "$\Delta P_{13}(t)$" brings to light the intervention of the battery B_2 and the battery B_3 (with charge or discharge operations). The power transition from "$\Delta P_{13}(t)$" to "$\Delta P_{14}(t)$" points out the grid intervention (injection or absorption). Then, the power

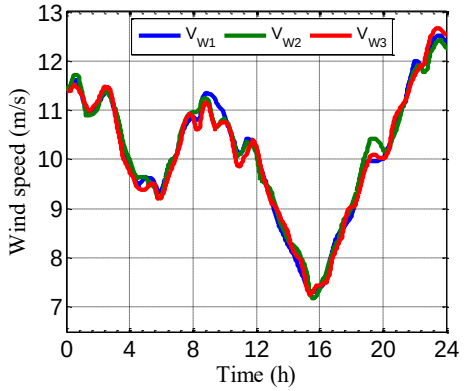

Fig.3. Wind speed in MGS 1, 2 and 3.

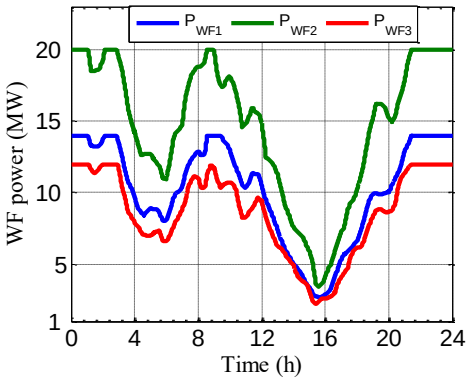

Fig.4. WF power in MGs 1, 2 and 3.

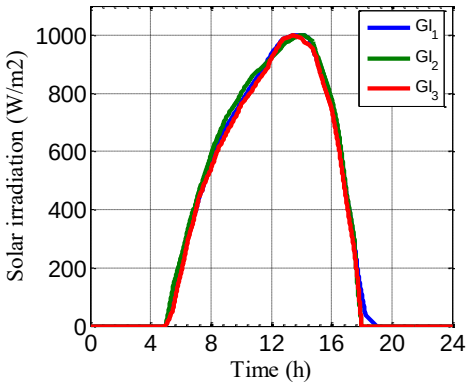

Fig.5. Solar irradiation in MGs 1, 2 and 3.

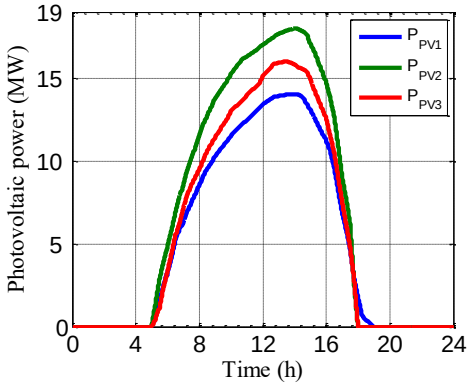

Fig.6. Photovoltaic power in MGs 1, 2 and 3.

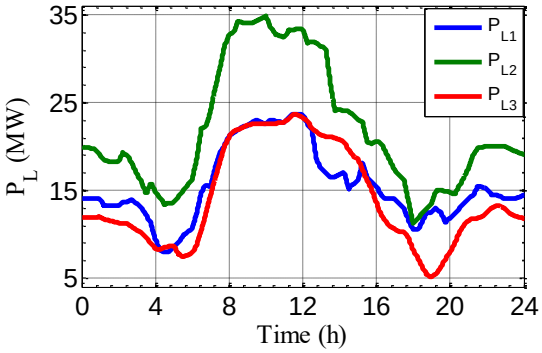

Fig.7. Load demand powers of MGs 1, 2 and 3.

transition from "$\Delta P_{14}(t)$" to "$\Delta P_{1f}(t)$" is made visible in case of lack of power or excess of power. In case of lack of power, this power transition shows either the grid intervention for supplying the HPL_1 and a set of LPL_1 while the rest of it is disconnected, or the grid and the DG_1 intervention for supplying the HPL_1 while all the LPL_1 is disconnected. In case of excess of power, this power transition points out the damping load operation.

The power variation assessment of MG_1 shows that after every change in RES supply or load, power variation in MG_1 is regulated to zero in order to maintain the equilibrium between production and consumption power in MG_1.

Transitions between the eleven modes of the MG_1 during the whole day are shown in Fig. 10 and it is noted that, at each moment, only one mode is active. It is shown in that figure that whatever change in RES supply or energy demanded by loads in MG_1, the proposed approach offers many power flow possibilities to monitor the MG_1 in the eleven modes and the energy demanded by loads is supplied by the RES_1.

In case of lack of power, the required power is compensated by one of the following possibilities :

- the power excess generated by the RES of neighboring MGs 2 and 3 (mode 1)
- the discharge operation of its own battery B_1 (mode 2)
- the discharge operation of its neighboring batteries B_2 and B_3 (mode 3)
- the supply of the main grid without disturbing the grid stability (mode 4)

- the grid supply of HPL_1 and a set of LPL_1while the rest LPL_1 is disconnected (mode 5)
- the supply of the HPL_1 by grid and DG_1 while all the LPL_1 is disconnected (mode 6).

In case of power excess, the equilibrium between production and consumer demand power is maintained by one of the following possibilities :

- meeting the needed power required by the neighboring MGs 2 and 3 (mode 7)
- charging its own battery B_1 (mode 8)
- charging its neighboring batteries B_2 and B_3 (mode 9)
- injecting the power excess into the grid without disturbing the grid stability (mode 10)
- sending the power excess to the dump load (mode 11).

In order to reveal the power path chosen for the MG_2 to ensure its power equilibrium between production and

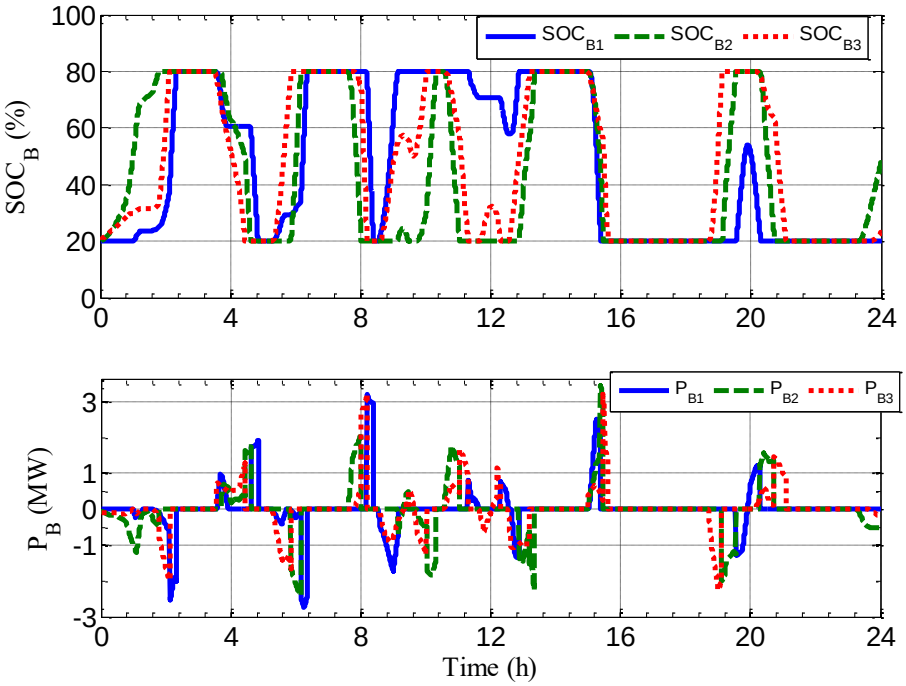

Fig.8. The battery states of charge and the battery powers of MGs 1, 2 and 3.

consumer demand, Fig. 11 shows the power variation assessment ("$\Delta P_2(t)$" → "$\Delta P_{20}(t)$" → "$\Delta P_{21}(t)$" → "$\Delta P_{22}(t)$" → "$\Delta P_{23}(t)$" → "$\Delta P_{24}(t)$" → "$\Delta P_{2f}(t)$"). The power transition from "$\Delta P_2(t)$" to "$\Delta P_{20}(t)$" points out the participation of the MG_2 (with its RES power excess or its required power) in maintaining the power equilibrium between production and consumption of the MG_1 and consequently reducing the gap of power between production and consumption in MG2 . The power transition from "$\Delta P_{20}(t)$" to "$\Delta P_{21}(t)$" points out the intervention of the neighboring MG_3 (with its RES power excess or its required power). The neighboring MG_1 (with their RES power excess or their required power) don't participate in the power equilibrium of the MG_2 in order not to disturb its equilibrium power already maintained between production and consumption by the power management algorithm. The power transition from "$\Delta P_{21}(t)$" to "$\Delta P_{22}(t)$" shows the intervention of the battery B_2 (with charge or discharge operations). The power transition from "$\Delta P_{22}(t)$" to "$\Delta P_{23}(t)$" reveals the intervention of the battery B_3 and the battery B_1 (with charge or discharge operations). The power transition from "$\Delta P_{23}(t)$" to "$\Delta P_{24}(t)$" points out the grid intervention(injection or absorption). Then, the power transition from "$\Delta P_{24}(t)$" to "$\Delta P_{2f}(t)$" shows clearly the equilibrium maintained between production and consumption power in case of lack of power or excess of power. In case of lack of power, this power transition is made visible whether after the grid intervention for supplying the HPL_2 and a set of LPL_2 while the rest of it is disconnected, or after the grid and the DG_2 intervention for supplying all the HPL_2 while all the LPL_2 is disconnected. In the case of excess of power, this power transition points out the damping load operation.

The power variation assessment of MG_2 reveals that after every change in RES supply or load, power variation in MG_2 is regulated to zero in order that the equilibrium between production and consumption power in MG_2 is maintained.

Similarly to the MG_1, the proposed supervision algorithm principal is applied to the MG_2. It allows getting the operating modes (1, 2, 3, 4, 7, 8, 9, 10, 11) which are illustrated in Fig. 12.

To display the power path chosen for the MG_3 to ensure its power equilibrium between production and consumer demand, Fig. 13 illustrates the power variation assessment ("$\Delta P_3(t)$" → "$\Delta P_{30}(t)$" → "$\Delta P_{32}(t)$" → "$\Delta P_{33}(t)$" → "$\Delta P_{34}(t)$" → "$\Delta P_{3f}(t)$"). The power transition from "$\Delta P_3(t)$" to "$\Delta P_{30}(t)$" shows the participation of the MG_3 (with its RES power excess or its required power) in maintaining the power equilibrium between production and consumption of the MGs 1 and 2 and consequently reducing the gap of power between production and consumption in MG_3. The neighboring MGs 1 and 2 (with their RES power excess or

their required power) don't participate in the power equilibrium of the MG_3 in order not to disturb their equilibrium power already maintained between production and consumption power by the power management algorithm. So, the algorithm moves to examine the intervention of the battery B_3 (with charge or discharge operations) which is observed according to the power transition from "$\Delta P_{30}(t)$" to "$\Delta P_{32}(t)$". The power transition from "$\Delta P_{32}(t)$" to "$\Delta P_{33}(t)$" shows the intervention of the battery B_2 and the battery B_1 (with charge or charge operations). The power transition from "$\Delta P_{33}(t)$" to "$\Delta P_{34}(t)$" proves the grid intervention (injection or absorption). Finally, the power transition from "$\Delta P_{34}(t)$" to "$\Delta P_{3f}(t)$" confirms the equilibrium maintained between production and consumption power in case of lack of power or excess of power. In case of lack of power, this power transition shows either the grid intervention for supplying the HPL_3 and a set of LPL_3 while

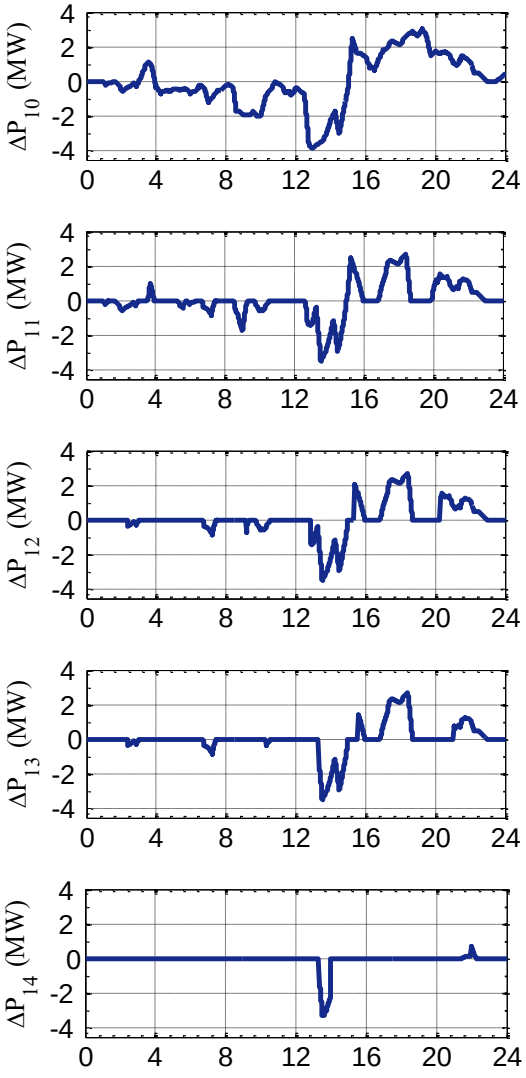

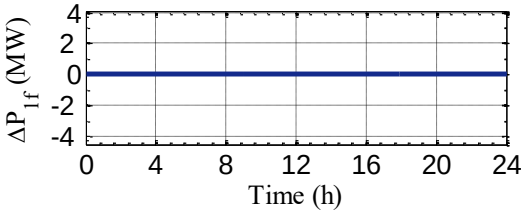

Fig.9. Power variation assessment of MG_1.

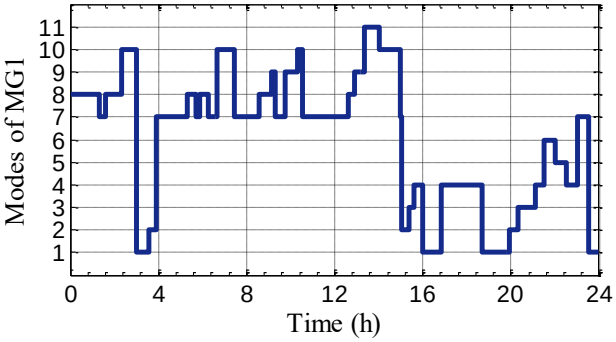

Fig.10. Operating modes of MG_1.

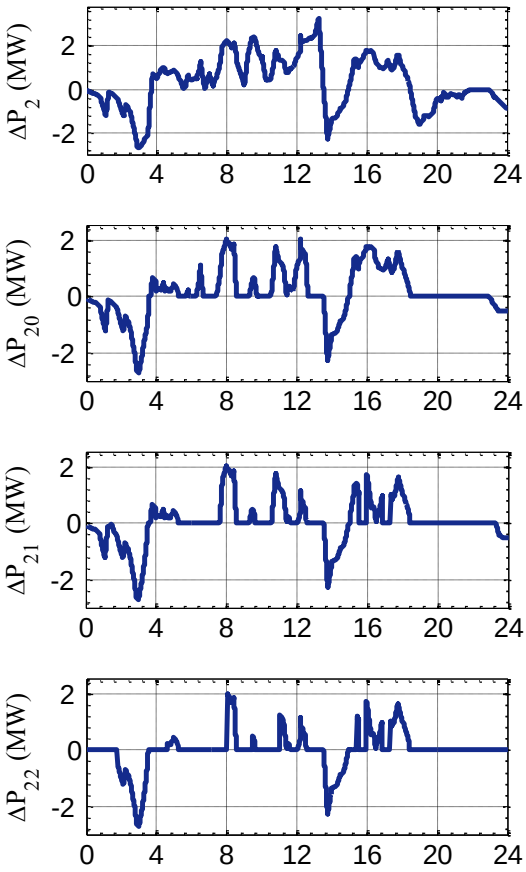

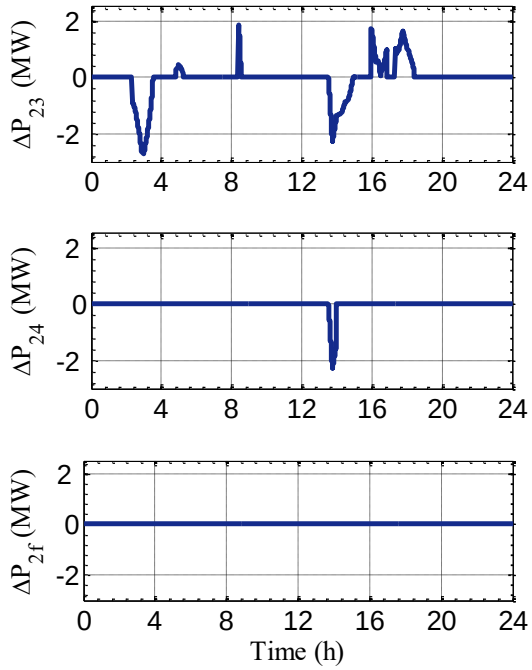

Fig.11. Power variation assessment of MG 2.

the rest of it is disconnected, or the grid and the DG_3 intervention for supplying the HPL_3 while all the LPL_3 is disconnected. In case of excess of power, this power transition makes visible the damping load operation.

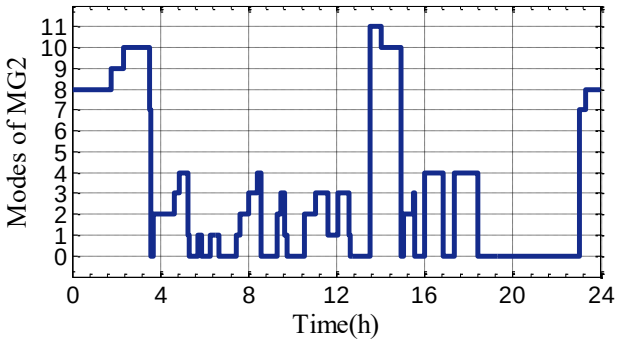

Fig.12. Operating modes of MG_2.

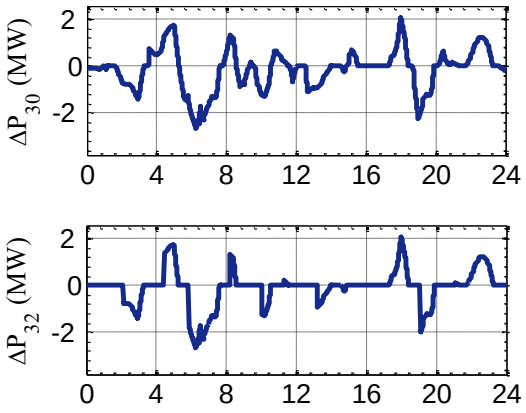

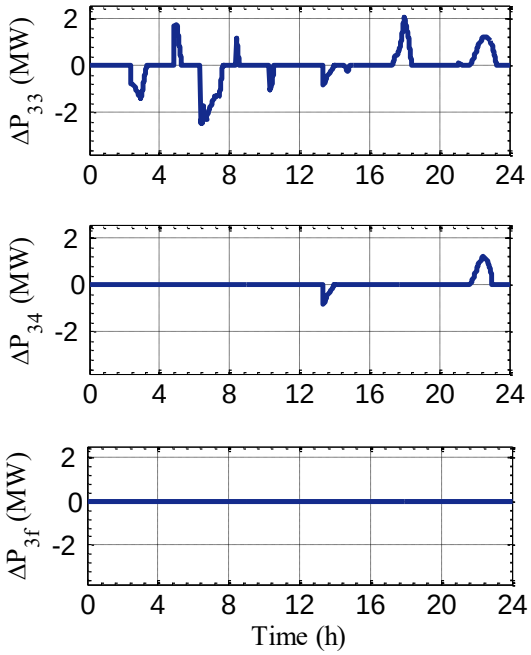

Fig.13. Power variation assessment of MG_3.

The power variation assessment of MG_3 shows that after every change in RES supply or load, power variation in MG_3 is regulated to zero so that the equilibrium between production and consumption power in MG_3 is obtainable.

Similarly to the MG_1 and MG_2, the proposed supervision algorithm principle is applied to the MG_3. It allows getting

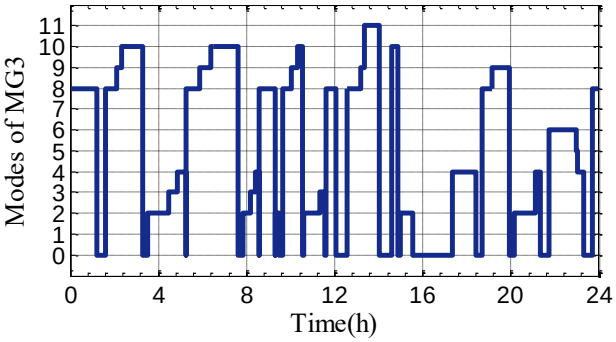

Fig.14. Operating modes of MG_3.

Table 1. Details of distributed energy resources in each MG of the studied system.

MGs	P_{PV} (MW)	P_{WF} (MW)	P_B (MW)	P_{DG} (MW)
MG 1 (30 MW)	14	14	1	1
MG 2 (40 MW)	18	20	1	1
MG 3 (30 MW)	16	12	1	1

Table 2. Specification of the wind turbines.

Parameters	Value
Power rated (MW)	2

V_c (m/s)	6
V_r (m/s)	11.2
V_f (m/s)	30

Table 3. Specification of the PV module.

Parameters	Value
Type	Monocristalline silicon
Nominal peak power (W)	280
Reference effeciency (%)	16.9
Optimum operating voltage (V_{mp})	32.4
Optimum operating current (I_{mp})	8.68
Open circuit voltage (V)	38.6
Short-circuit current (A)	9.37
N_{oct} (C°)	46.5
Dimensions	1625×1019×46 mm

Table 4. Specification of Li-ion battery cell(3.3V, 2.3A h).

Parameters	Value
Battery constant voltage	3.366 V
Internal resistance	0.01 Ω
Constant Polarization	0.0076 Ω
Exponential zone amplitude	0.26422 V
Exponential zone inverse constant time	26.5487 $(Ah)^{-1}$
Battery cell energy	7.59 Wh
Minimum SOC limit	20%
Maximum SOC limit	80%

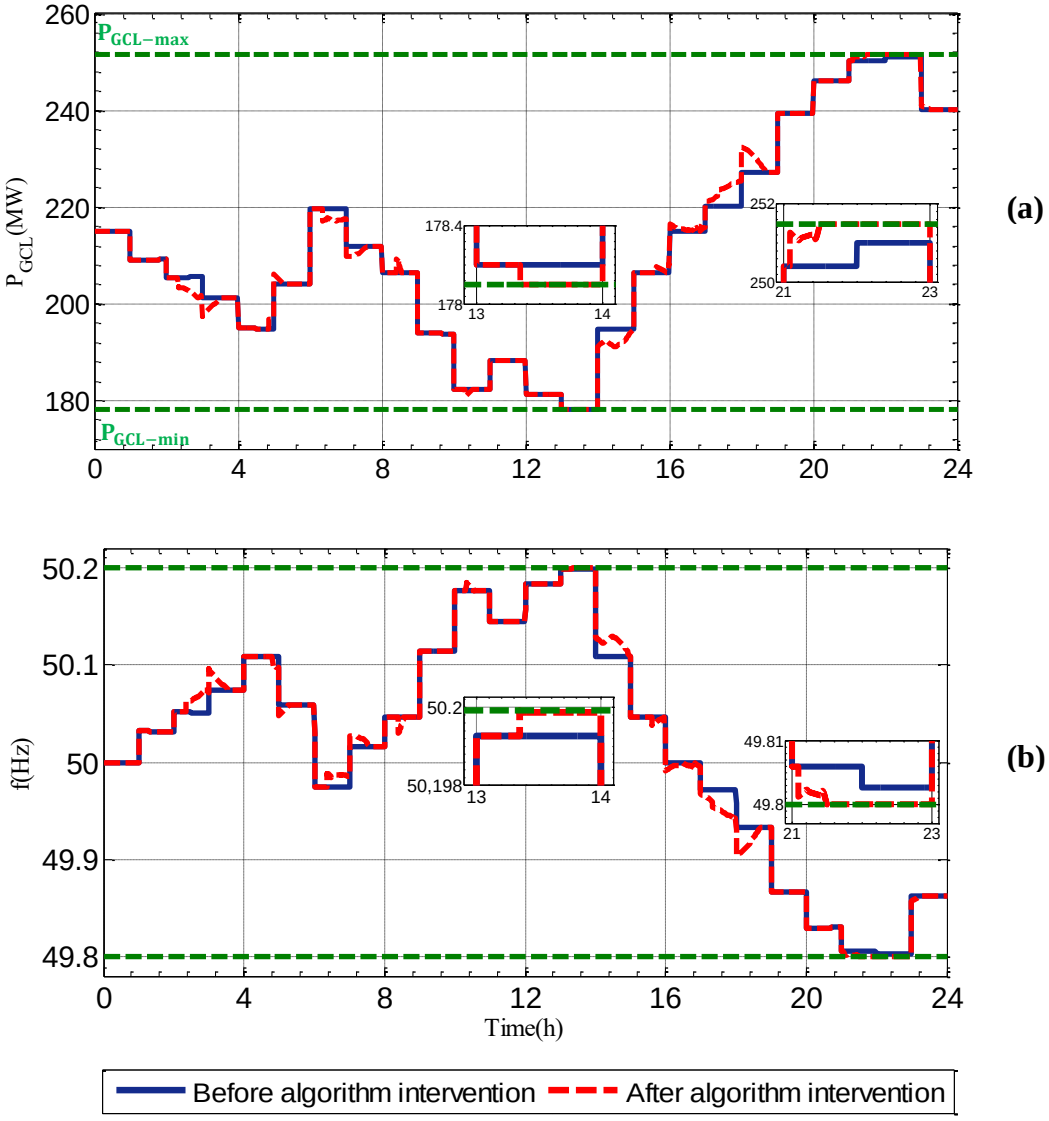

Fig.15. "Power dispatching" algorithm impact on the grid frequency: power of grid connected loads after algorithm intervention (a) and grid frequency after algorithm intervention (b).

the operating modes (2, 3, 4, 5, 6, 8, 9, 10, 11) which are illustrated in Fig. 14.

From fig. 15a, it is observable that the power of grid connected loads before and after algorithm intervention

doesn't exceed power limits "P_{GCL_min}" and "P_{GCL_max}". Figure 15b shows the grid frequency after algorithm intervention (modes 4, 5, 6, 10 and 11). It is observable that the grid frequency variation does not exceed its desired margins after grid participation in maintaining equilibrium between production and consumption power of MGs.

Conclusion

This article presents a power dispatching algorithm addressing the power flow between MGs. This algorithm ensures the managing of multi-input energy sources with the consideration of the load demand and also the dispatch of the power exchanged among the neighboring MGs and the main grid. MGs can operate either in an islanded mode when the internal loads are fed with the MG's own hybrid system or with the neighboring MG's hybrid system, or in grid-connected mode when the MG is connected to the main grid. The equilibrium between production and consumption power in each MG is ensured through power exchanging between the neighboring MGs as well as the main grid. Simulation results are presented to show the reliability of the proposed power dispatching strategy.

References

[1] M. L. Tuballa, and M. L. Abundo, "A review of the development of Smart Grid technologies", *Renewable and Sustainable Energy Reviews*, vol. 59, pp. 710-725, 2016.

[2] K. Zhou, S. Yang, Z. Chen, and S. Ding, "Optimal load distribution model of microgrid in the smart grid environment", *Renewable and Sustainable Energy Reviews*, vol. 35, pp. 304-310, 2014.

[3] Y. Yoldas, A. Önen, S. M. Muyeen, A. V. Vasilakos, and I. Alan, "Enhancing smart grid with microgrids: Challenges and opportunities", *Renewable and Sustainable Energy Reviews*, vol. 72, pp. 205-214, 2017.

[4] A. H. Fathima, and K. Palanisamy, "Optimization in microgrids with hybrid energy systems – A review", *Renewable and Sustainable Energy Reviews*, vol. 45, pp. 431-446, 2015.

[5] Q. Jiang, M. Xue, and G. Geng, "Energy management of microgrid in grid-connected and stand-alone modes", *IEEE Transactions On Power Systems*, vol. 28, pp. 3380-3389, 2013.

[6] L. Meng, E. R. Sanseverino, A. Luna, T. Dragicevic, J. C. Vasquez, and J. M. Guerrero, "Microgrid supervisory controllers and energy management systems: A literature review", *Renewable and Sustainable Energy Reviews*, vol. 60, pp. 1263-1273, 2016.

[7] Z. Li, and Y. Xu, "Optimal coordinated energy dispatch of a multi-energy microgrid in gridconnected and islanded modes", *Applied Energy*, vol. 210, pp. 974-986, 2017.

[8] Y. Zhang, N. Gatsis, and G. B. Giannakis, "Robust energy management for microgrids with high-penetration renewables", *IEEE Transactions On Sustainable Energy*, vol. 4, pp. 944-953, 2013.

[9] T. C. Ou, and C. M. Hong, "Dynamic operation and control of microgrid hybrid power systems", *Energy*, vol. 66, pp. 314-323, 2014.

[10] W. Shi, X. Xie, C.C. Chu, and R. Gadh, "Distributed Optimal Energy Management in Microgrids", *IEEE Transactions On Smart Grid*, vol. 6, pp. 1137-1146, 2015.

[11] S. Kirmani, M. Jamil, and I. Akhtar, "Bi-directional power control mechanism for a microgrid hybrid energy system with power quality enhancement capabilities", *International journal of renewable energy research*, vol. 7, pp. 1962-1969, 2017.

[12] L. H. Koh, P. Wang, F. H. Choo, K. J. Tseng, Z. Y. Gao, and H. B. Püttgen, "Operational Adequacy Studies of a PV-Based and Energy Storage Stand-Alone Microgrid", *IEEE Transactions On Power Systems*, vol. 30, pp. 892-900, 2015.

[13] C. Wang, Y. Liu, X. Li, L. Guo, L. Qiao, and H. Lu, "Energy management system for stand-alone diesel-wind-biomass microgrid with energy storage system", *Energy*, vol. 97, pp. 90-104, 2016.

[14] J. Pascual, J. Barricarte, P. Sanchis, and L. Marroyo, "Energy management strategy for a renewable-based residential microgrid with generation and demand forecasting", *Applied Energy*, vol. 158, pp. 12-25, 2015.

[15] A. Nadimi, and F. Adabi, "Optimized planning for hybrid microgrid in grid connected mode", *International journal of renewable energy research*, vol. 6, pp. 494-503, 2016.

[16] H. Kanchev, F. Colas, V. Lazarov, and B. Francois, "Emission reduction and economical optimization of an urban microgrid operation including dispatched PV-based active generators", *IEEE Transactions On Sustainable Energy*, vol. 5, pp. 1397-1405, 2014.

[17] M. Marzband, A. Sumper, A. R. Álvarez, J. L. D. García, and B. Tomoiaga, "Experimental evaluation of a real time energy management system for stand-alone microgrids in day-ahead markets", *Applied Energy*, vol. 106, pp. 365-376, 2013.

[18] M. Marzband, M. Ghadimi, A. Sumper, and J. L. D. García, "Experimental validation of a real-time energy management system using multi-period gravitational search algorithm for microgrids in islanded mode", *Applied Energy*, vol. 128, pp. 164-174, 2014.

[19] B. Belvedere, M. Bianchi, A. Borghetti, C. A. Nucci, M. Paolone, and A. Peretto, "A microcontroller-based power management system for standalone microgrids with hybrid power supply", *IEEE Transactions On Sustainable Energy*, vol. 3, pp. 422-431, 2012.

[20] S. Tan, J. X. Xu, and S. K. Panda, "Optimization of distribution network incorporating distributed generators: An integrated approach", *IEEE Transactions On Power Systems*, vol. 28, pp. 2421-2432, 2013.

[21] X. Lu, J. Wang, and L. Guo, "Using microgrids to enhance energy security and resilience", *The Electrical Journal*, vol. 29, pp. 8-15, 2016.

[22] X. Fang, S. Ma, Q. Yang, and J. Zhang, "Cooperative energy dispatch for multiple autonomous microgrids with distributed renewable sources and storages", *Energy*, vol. 99, pp. 48-57, 2016.

[23] M. Fathi, and H. Bevrani, "Statistical cooperative power dispatching in interconnected microgrids", *IEEE*

Transactions On Sustainable Energy, vol. 4, pp. 586-593, 2013.

[24] D. Gregoratti, and J. Matamoros, "Distributed energy trading: The multiple-microgrid case", *IEEE Transactions On Industrial Electrical*, vol. 62, pp. 2551-2259, 2014.

[25] Z. Wang, B. Chen, J. Wang, and J. Kim, "Decentralized energy management system for networked microgrids in grid-connected and islanded modes", *IEEE Transactions On Smart Grid*, vol. 7, pp. 1097-1105, 2015.

[26] H. Haddadian, and R. Noroozian, "Multi-microgrids approach for design and operation of future distribution networks based on novel technical indices", *Applied Energy*, vol. 185, pp. 650-663, 2017.

[27] M. Rekik, A. Abdelkafi, and L. Krichen, "A micro-grid ensuring multi-objective control strategy of a power electrical system for quality improvement", *Energy*, vol. 88, pp. 1-13, 2015.

[28] S. Ruiz-Alvarez, J. Patino, A. Marquez, and J. Espinoza, "Optimal design for an electrical hybrid microgrid in colombia under fuel price variation", *International*

[34] A. M. Kassem, and A. M. Yousef, "Robust control of an isolated hybrid wind–diesel power system using Linear Quadratic Gaussian approach", *International Journal of Electrical Power & Energy Systems*, vol. 33, pp. 1092-1100, 2011.

journal of renewable energy research, vol. 7, pp. 1535-1545, 2017.

[29] S. Diaf, D. Diaf, M. Belhamel, and M. Haddadi, "A methodology for optimal sizing of autonomous hybrid PV/wind system", *Energy Policy*, vol. 35, pp. 5708-5718, 2017.

[30] H. Belmili, M. Haddadi, S. Bacha, M.F. Almi, and M. Bendib, "Sizing stand-alone photovoltaic-wind hybrid system: Techno-economic analysis and optimization", *Renewable and Sustainable Energy Reviews*, vol. 30, pp. 821-832, 2014.

[31] O. Tremblay, and L. Dessaint, "Experimental validation of a battery dynamic model for EV applications", *World Electric Vehicle*, vol. 3, pp. 289-298, 2009.

[32] H. Rahimi-Eichi, and M.Y. Chow, "Adaptive Parameter Identification and State-of-Charge Estimation of Lithium-Ion Batteries", *IECON Conference*, Montreal, pp. 4012-4017, 25-28 Oct, 2012.

[33] T. Balamurugan, and S. Manoharan, "Optimal Power Flow Management Control for Grid Connected Photovoltaic/Wind turine/Diesel generator (GCPWD)

[35] M. S. Ismai, M. Moghavvemi, and T. M. I. Mahlia, "Techno-economic analysis of an optimized photovoltaic and diesel generator hybrid power system for remote houses in a tropical climate", *Energy Conversion and Management*, vol. 69, pp. 163-173, 2013.

Nomenclature

V_i	wind speed applied to each WT (m/s)	I	battery current (A)
n_T	number of WT units	i.t	actual battery charge (Ah)
V_c	cut-in wind speed (m/s)	i^*	battery filtered current (A)
V_F	cut-off wind speed (m/s)	K	constant polarization
V_R	rated wind speed (m/s)	Q	battery capacity (Ah)
P_{Wr}	WT rated power (KW)	A	exponentiel zone amplitude (V)
N_{PV}	number of PV	B	exponentiel zone inverse constant time ($(Ah)^{-1}$)
GI	global solar irradiation ($W.m^2$)	SOC_{min}	minimum value of the battery SOC
T_c	solar cell temperature (°C)	SOC_{max}	maximum value of the battery SOC
T_{cref}	reference solar cell temperature (°C)	τ_C	the fuel combustion delay
T_a	ambient temperature (°C)	τ_d	the ignition retard
A_{PV}	PV generator surface	F	the fuel level gain.
N_{oct}	nominal operating cell temperature (°C)	P_{GCL}	the demanded power by the grid connected load
U_0	battery constant voltage (V)	$P_{GCL-min}$	the demanded power from the grid connected load at the PCC corresponding to the frequency 50.2
R	battery internal resistance (Ω)	$P_{GCL-max}$	the demanded power from the grid connected load at the PCC corresponding to the frequency 49.8